



Mechanical properties of cubic zirconia irradiated with swift heavy ions

V. Menvie Bekale^a, G. Sattonnay^{a,*}, C. Legros^a, A.M. Huntz^a, S. Poissonnet^b, L. Thomé^c

^a Université Paris-Sud, LEMHE/ICMMO, UMR 8182, Bâtiment 410, F-91405 Orsay cedex, France

^b DEN/DANS/DMN/SRMP, CEA Saclay, 91191 Gif-sur-Yvette cedex, France

^c Centre de Spectrométrie Nucléaire et de Spectrométrie de Masse, CNRS/IN2P3/Université Paris-Sud, Bâtiment 104-108, F-91405 Orsay cedex, France

ARTICLE INFO

Article history:

Received 27 August 2008

Accepted 21 October 2008

ABSTRACT

The modifications of the mechanical properties of cubic (yttria-stabilized) zirconia induced by swift heavy ion irradiation are investigated. Polycrystalline pellets were irradiated at room temperature with 940 MeV Pb ions at the GANIL accelerator in Caen at fluences ranging from 5×10^{11} to $4 \times 10^{13} \text{ cm}^{-2}$. The microhardness and the fracture toughness of irradiated YSZ were studied by Vickers micro-indentation. Although YSZ is damaged by irradiation, an increase of the microhardness and fracture toughness with increasing ion fluence is observed. A strengthening of YSZ, associated with residual compressive stresses induced in the surface layer by irradiation, explain these results.

© 2008 Elsevier B.V. All rights reserved.

1. Introduction

Cubic yttria-stabilized zirconia (YSZ) is considered as one of the most promising materials for use as an inert matrix for the transmutation or storage of actinides produced in nuclear power plants [1–6]. This high-temperature refractory oxide is attractive because it presents a high chemical durability, an excellent radiation stability and an ability to form solid solutions with actinide elements (Pu, U, Th) in a wide concentration range [7–9].

Nuclear fuel matrices are exposed to severe radioactive environments, mainly due to neutron exposure and heavy fission-fragment damage, which may induce structural and microstructural transformations leading to drastic modifications of the materials properties. Radiation-induced defects can potentially affect the mechanical properties of a material by producing embrittlement or microcracking. Whereas the effects of nuclear collisions investigated by low-energy ion irradiation are relatively well-understood [5,10–14], the effects of severe electronic excitations arising from irradiation with high-energy ions was yet very little studied. Moreover, the literature data on the mechanical properties of ion-irradiated zirconia are rather limited [15–17].

The present work deals with the effect of both the grain size of pellets and the slowing-down of swift heavy ions on the mechanical properties of YSZ ceramics. The modifications of the mechanical properties were investigated by indentation techniques, which allowed us to determine both the hardness and the toughness of samples. The various results are discussed in the light of the durability of the material.

2. Experimental

YSZ polycrystals with 10 mol% Y_2O_3 (10YSZ) were synthesized from the process retained and described in a previous paper [18]. In summary, zirconia powder supplied by Tosoh Co. Ltd. (Tokyo, Japan) was pressed at 250 MPa with a cold isostatic press and then sintered at 1450 °C for 5 h or 168 h in air. Samples cut from pellets and mechanically polished were annealed at 1400 °C for 10 h in air in order to remove polishing damage and also to reveal grain boundaries (thermal etching). The sintering at 1450 °C for 5 h led to a relative density of 98.4% with an average grain size of 3.5 μm (ranging from 2 to 5 μm as shown in Fig. 1(a)). For the longer sintering time (168 h), a ceramic with a relative density of 99.5% is obtained with an average grain size of 6 μm (ranging from 2 to 10 μm as shown in Fig. 1(b)).

Polycrystals were irradiated at room temperature with 940 MeV Pb ions at the GANIL accelerator in Caen, at fluences ranging from 5×10^{11} to $4 \times 10^{13} \text{ cm}^{-2}$. Fig. 2 presents the variation of the electronic (S_e) and nuclear (S_n) energy losses as a function of the depth in YSZ irradiated with 940 MeV Pb ions (calculated with the TRIM code [19]). These plots clearly show that S_e overwhelms S_n by several orders of magnitude when the values are averaged over the first micrometer (in this case $S_e = 44.5 \text{ keV nm}^{-1}$ and $S_n = 0.1 \text{ keV nm}^{-1}$). The projected range (R_p) of Pb ions is 28 μm. X-ray diffraction (XRD) measurements show that the irradiated layer remains crystalline (cubic fluorite-type structure) whatever the 940 MeV Pb ions fluence [20].

Scanning electron microscopy (SEM) experiments were carried out with a Zeiss Supra VP55 equipped with a field emission gun. Observations of the outer surface of samples by SEM allowed us both to determine their microstructure (mainly the grain size), and to accurately observe the indentation prints and the morphology of cracks.

* Corresponding author.

E-mail address: gael.sattonnay@u-psud.fr (G. Sattonnay).

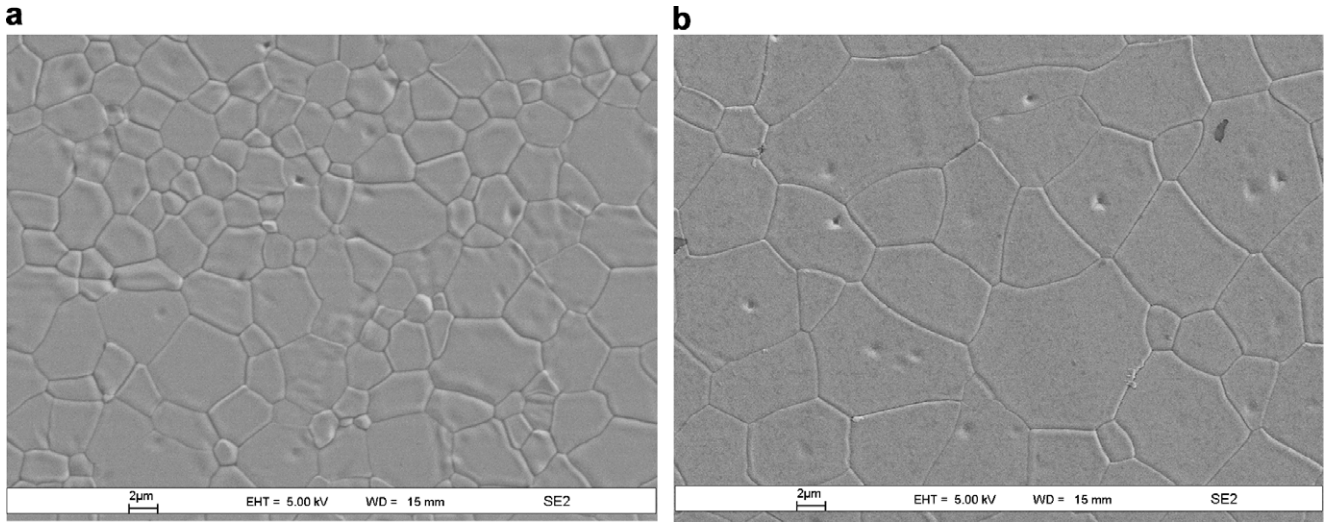


Fig. 1. SEM micrographs of polished and thermal etched surfaces of YSZ polycrystals after sintering at 1450 °C for 5 h (a) and 168 h (b).

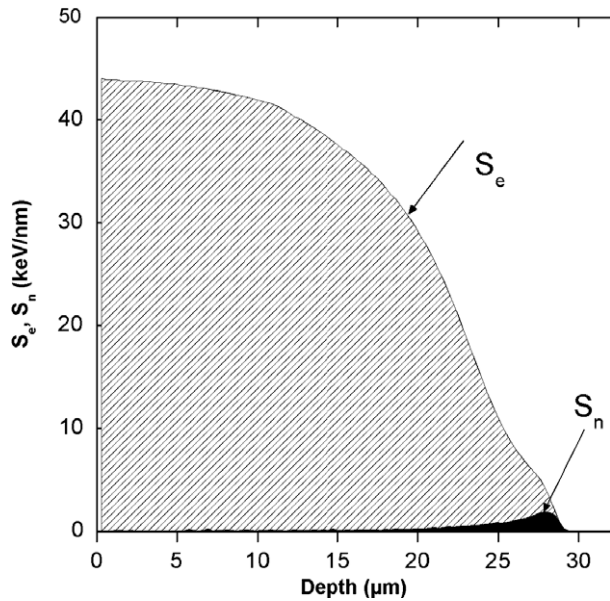


Fig. 2. Electronic (S_e) and nuclear (S_n) energy losses in YSZ versus depth for 940 MeV Pb irradiation. Calculations were performed with the TRIM code [19].

Vickers indentations were made on polished samples using a LECO M-400-H hardness testing machine with a maximum load of 0.5 N held for 15 s. For each specimen, 10 tests were conducted with a space of 0.05 mm between indents. The maximum indentation depth was estimated to be $\sim 1.6 \mu\text{m}$. The Vickers microhardness (HV) was deduced from the diagonal length ($2a$) of the indentation print and the contact load (P) by the following equation [21]:

$$\text{HV} = 1.854 \frac{P}{(2a)^2}. \quad (1)$$

For fracture toughness (K_{IC}) calculations, a maximum load of 10 N was used in order to produce cracks. The average crack length (c) was measured with an optical microscope combined to a hardness testing machine (see Fig. 3). The distance between indents was estimated to be of the order of 150 μm . K_{IC} was derived from the equation proposed by Anstis et al. [22] for half-penny cracks:

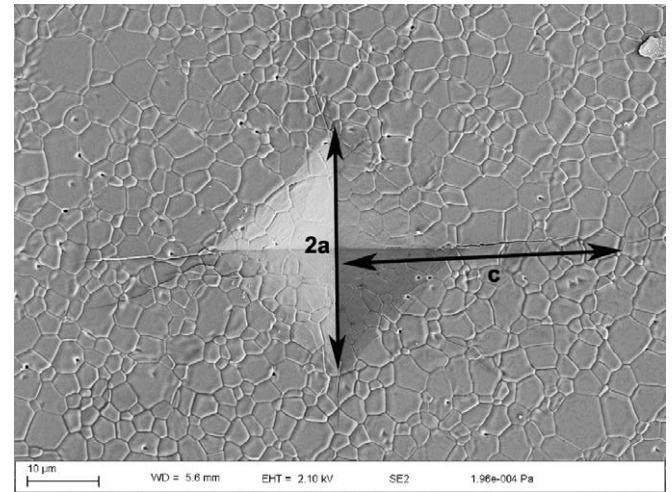


Fig. 3. SEM micrograph of an indent (load = 10 N). Definition of the diagonal length ($2a$) and of the fracture length (c) used in Eqs. (1) and (2).

$$K_{IC} = 0.0154 \left(\frac{E}{\text{HV}} \right)^{1/2} \frac{P}{c^{3/2}}, \quad (2)$$

where E is the elastic modulus of the material, which is determined from nano-indentation measurements using a Berkovich indenter (20 indents for each sample with a load in a 0–500 mN range and a maximum indentation depth of 1500 nm) and the Oliver and Pharr method [23]. Actually, nano-indentation measurements give the reduced Young modulus (E_r). The Young modulus of the material (E) is thus obtained by the equation [24]:

$$\frac{1}{E_r} = \frac{1 - \nu^2}{E} + \frac{1 - \nu_i^2}{E_i}, \quad (3)$$

where E_i and ν_i are the Young modulus and the Poisson ratio of the indenter ($E_i = 1141 \text{ GPa}$ and $\nu_i = 0.07$), respectively. According to Eigenmann et al. [25], the Poisson ratio of cubic zirconia (ν) was taken as 0.29.

3. Results

Fig. 4(a) presents the variation of the Vickers microhardness (HV) as a function of the ion fluence and of the average grain size

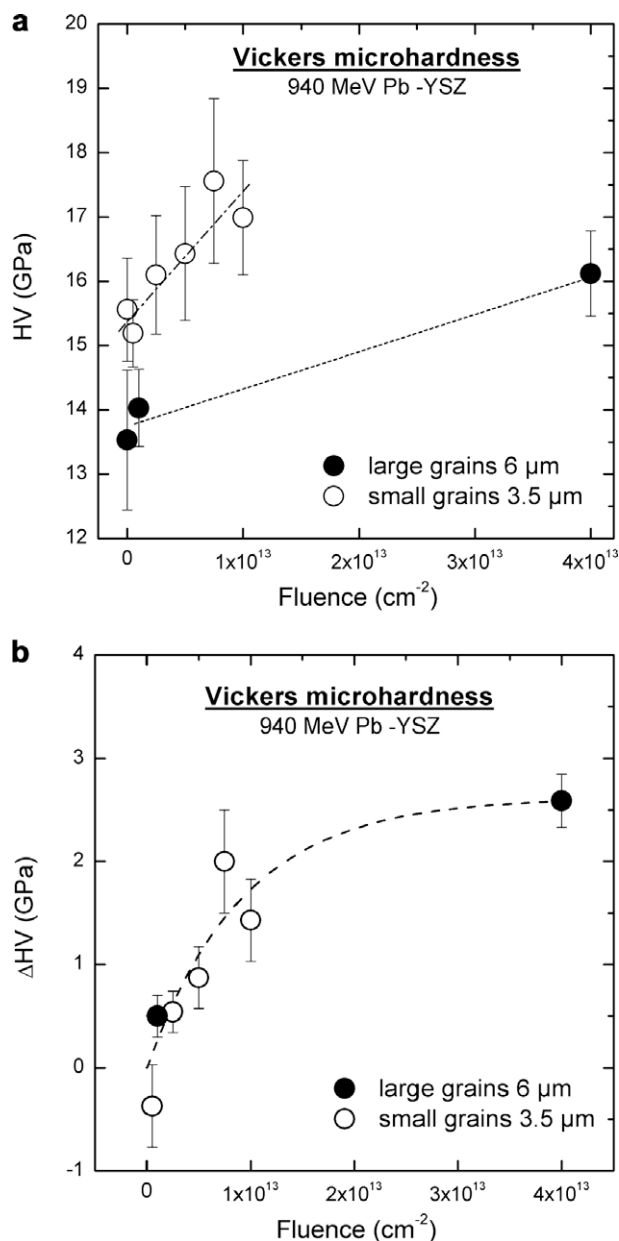


Fig. 4. Absolute (a) and relative (b) Vickers microhardness versus ion fluence for YSZ (with different grain sizes) irradiated with 940 MeV Pb ions.

in 10YSZ polycrystals. For pristine polycrystals the microhardness of samples with small grains (15.5 GPa) is greater than that of samples with large grains (13.5 GPa). For irradiated polycrystals an increase of the microhardness with increasing ion fluence is observed. Thus, hardening is affected by both the grain size and the irradiation process. To suppress the effect of the initial microstructure, a relative microhardness is defined as $\Delta HV = HV_i - HV_0$, where HV_0 and HV_i are the microhardnesses of YSZ before and after irradiation, respectively. Thus, ΔHV should reflect only the variation of the hardness due to radiation effects. It is clearly seen on Fig. 4(b) that ΔHV depends only on the irradiation conditions and not on the grain size; it increases with increasing fluence up to a saturation value of 2.5 GPa.

By applying a strong load during Vickers micro-indentation tests, cracks have been created on the polished surface of samples. Fig. 5 presents SEM micrographs of indents performed on pristine and irradiated polycrystals. Fig. 5(a) shows an indent obtained by

applying a load of 4.9 N on a pristine sample with large grains. The indent is composed of long and open transgranular cracks which appear on the corners and, sometimes, on the edges of the indent. For irradiated samples, the applied load must be higher to produce cracks. An example of indent performed with a load of 10 N on an irradiated sample at a fluence of $5 \times 10^{12} \text{ cm}^{-2}$ is shown in Fig. 5(b). Transgranular cracks are also seen, but even when the highest load is used they are smaller than those observed on pristine sample. An erosion of the edge of indents is sometimes obtained from a fluence of 10^{13} cm^{-2} (see e.g. Fig. 5(c), and when the fluence increases the indent can totally collapse (Fig. 5(d)) just after the application of the load.

The fracture toughness deduced from Eq. (2) using measurements of half-penny cracks increases with the ion fluence (see the data for zero fluence in Fig. 6(a) and becomes slightly higher when the average grain size decreases (Fig. 6(a)). The effect of the initial microstructure was also suppressed by calculating a relative toughness defined as $\Delta K_{IC} = K_{ICi} - K_{IC0}$, where K_{IC0} and K_{ICi} are the fracture toughnesses of YSZ before and after irradiation, respectively. ΔK_{IC} increases with increasing ion fluence (Fig. 6(b)). The fracture toughness of sample irradiated at $4 \times 10^{13} \text{ cm}^{-2}$ cannot be determined because of the collapse of all indents. Thus, no saturation effect could be observed at high fluences.

Berkovitch nano-indentation tests conducted on pristine and irradiated polycrystals led to hardness values and variations similar to those of micro-indentation: the nanohardness increases with increasing ion fluence, the increase being higher when the average grain size is smaller (Fig. 7(a)). The value of the Young's modulus at the maximum indentation depth (1500 nm) is almost constant at ~ 200 GPa (Fig. 7(b)).

It is worth noting that the nanohardness and the microhardness of pristine polycrystals are close to the values given in the literature, i.e. ranging from 12 to 15 GPa. This is also the case for the Young's modulus for which most of reported values are included in a 200–220 GPa range [26–28].

4. Discussion

4.1. Influence of the microstructure

The values of microhardness determined on pristine 10YSZ polycrystals show that the hardness is dependent on the grain size and thus on the sample microstructure: the hardness of samples with small grains is 2 GPa higher than that of samples with large grains. According to the well-known Hall and Petch law, the increase of the yield strength (σ_Y) is inversely proportional to the square root of the grain size. Since the hardness is directly related to the yield strength through the equation: $HV = 3\sigma_Y$ [29], the hardening may be attributed to the higher grain boundary density when the grains are smaller.

The fracture toughness K_{IC} of irradiated polycrystals increases when the grain size decreases (Fig. 6(a)). The toughness of samples with small grains is $0.5 \text{ MPa m}^{1/2}$ higher than that of samples with large grains. As the cracks are of transgranular type, the grain boundaries are more resistant than the grains. Thus, the grain boundaries constitute obstacles to cracking. If the grain boundary density increases, the fracture toughness is higher, so that the cracking is slowed down.

Dahl et al. showed that, for 8YSZ polycrystals, the Vickers microhardness and the fracture toughness are almost similar whatever the grain size [28]. This result can be explained by the fact that zirconia prepared by different sintering techniques exhibits different porosities which could hide grain boundary effects in the case of samples with small grains. However, the values found by Dahl et al. for the microhardness (12.4–13.5 GPa) and for the

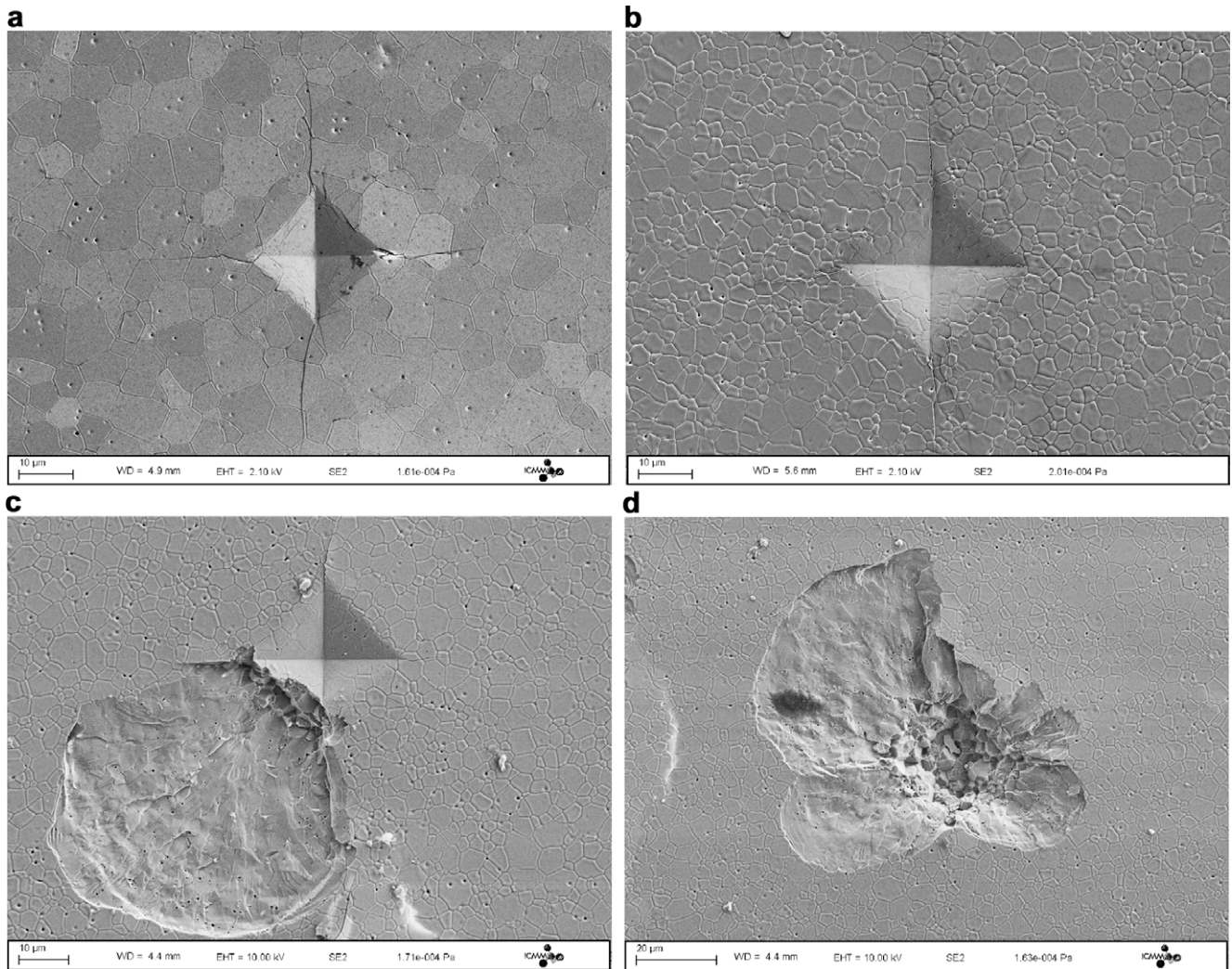


Fig. 5. SEM micrographs of typical indents on the polished and thermally etched surfaces of pristine YSZ (a) and 940 MeV Pb-irradiated YSZ at fluences of $5 \times 10^{12} \text{ cm}^{-2}$ (b), 10^{13} cm^{-2} (partially collapsed print) (c), and $4 \times 10^{13} \text{ cm}^{-2}$ (totally collapsed print) (d).

fracture toughness ($1.3\text{--}1.5 \text{ MPa m}^{1/2}$) are close to those determined on pristine polycrystals with large grains in the present study (13.5 GPa and $1.3 \text{ MPa m}^{1/2}$, respectively).

4.2. Effects of irradiation

The Vickers microhardness of YSZ polycrystals irradiated with 940 MeV Pb ions increases with increasing ion fluence whatever the microstructure of pellets (Fig. 4(a)). The same result is observed (Fig. 7(a)) in the case of the nanohardness at the maximum indentation depth (1500 nm). Despite the scattering of experimental values, the nanohardness of irradiated samples is always higher than (or equal to) that of pristine samples at high indentation depths ($\geq 200 \text{ nm}$). Sickafus et al. [15] have performed nano-indentation experiments on 9.5YSZ single crystals irradiated with low-energy ions (370 keV Xe), and they found that the nanohardness of irradiated samples did not significantly change with the ion fluence: the nanohardness increased by about 2 GPa after irradiation and it remained unchanged for high fluences. Nevertheless, the results of Sickafus et al. are hardly comparable with the present results: in the Sickafus experiments, irradiation was performed with low-energy ions at low temperature, whereas in our work irradiation was carried out with high-energy ions at room temperature. The defects and the microstructure changes produced during the two

types of irradiation are very likely too different to allow a direct comparison.

The relative microhardness of YSZ increases with increasing ion fluence up to a saturation value of 2–3 GPa (Fig. 4(b)). Similarly, even if no saturation effect is observed, the relative fracture toughness of YSZ shows an increase by about 2–2.5 $\text{MPa m}^{1/2}$ at a fluence of 10^{13} cm^{-2} (Fig. 6(b)). How are these results related to radiation effects? Recently, Moll et al. [30] have investigated, by Rutherford backscattering spectrometry and channelling (RBS/C), the damage build-up for 9.5YSZ single crystals irradiated with 940 MeV Pb ions. The fraction of atoms displaced from their original sites during irradiation (f_D) has been determined. An outstanding result arising from these experiments is that the variation of f_D with the ion fluence can be described by a single impact mechanism [30]. The saturation of the radiation damage is nearly reached at 10^{13} cm^{-2} . As the value of the microhardness is also saturated at this fluence, the variation of the microhardness can be correlated with the amount of defects produced by irradiation.

More surprising is the increase of the toughness of pellets with increasing ion fluence, although YSZ is severely damaged. Actually, radiation defects degrade the material, so that the toughness should decrease upon irradiation. In fact the strengthening of YSZ is only apparent; besides radiation defects, irradiation with an

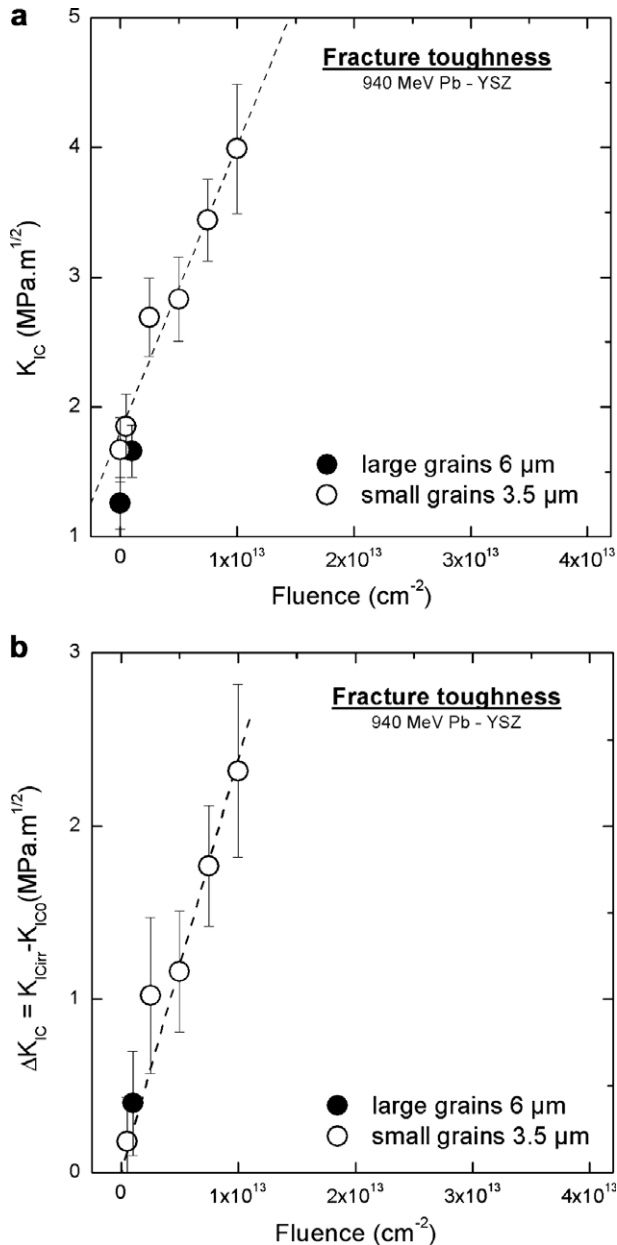


Fig. 6. Absolute (a) and relative (b) fracture toughness versus ion fluence for YSZ (with different grain sizes) irradiated with 940 MeV Pb ions.

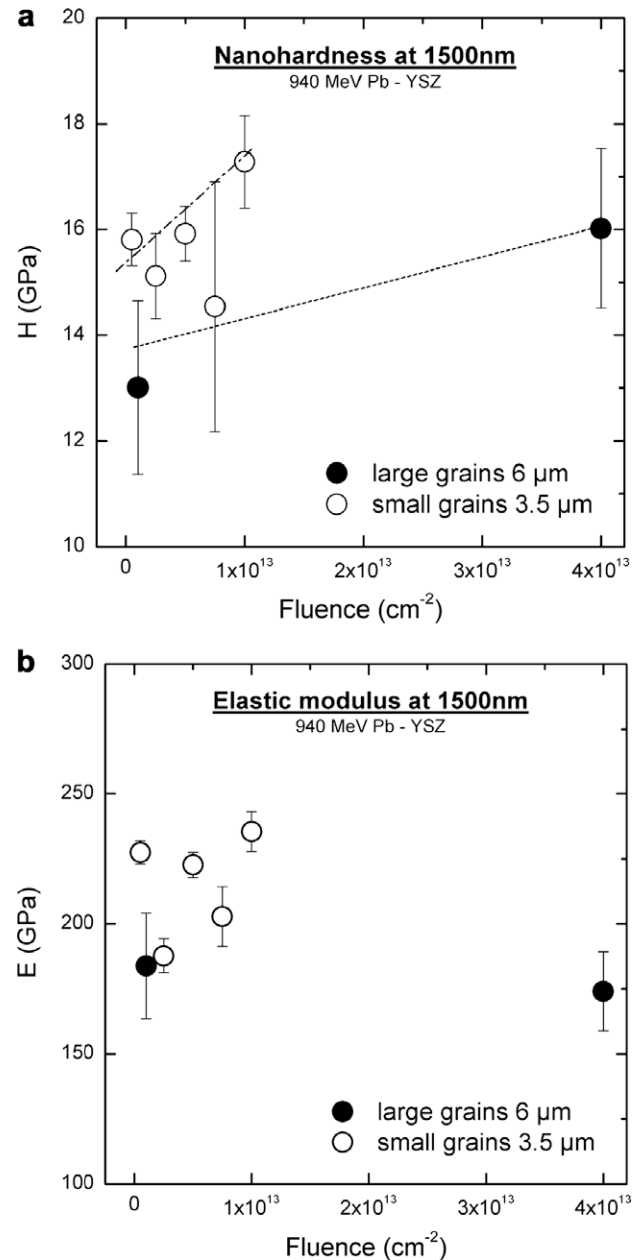


Fig. 7. Nanohardness (a) and elastic modulus measured at 1500 nm (b) versus ion fluence for YSZ (with different grain sizes) irradiated with 940 MeV Pb ions.

ion beam creates a residual stress field in the surface region of the target. In a previous paper [31], the residual stresses induced by irradiation on similar YSZ polycrystals irradiated with 940 MeV Pb ions were examined by XRD using the 'sin² ψ method'. The analysis of experimental data was performed by means of a triaxial stress model. Results showed that the lattice parameter increases with increasing ion fluence, which means that radiation defects lead to a swelling of the damaged layer and therefore generate a hydrostatic tensile stress ($\sigma_{hyd} > 0$). As the lateral dimensions of the damaged layer are imposed by the undamaged part of the material beneath the damaged part, a biaxial state of compressive stress ($\sigma_{bi} < 0$) is superimposed to the hydrostatic stress, according to the equation:

$$\sigma_{hyd} = -\beta\sigma_{bi} \quad (4)$$

The values of σ_{bi} and β (and thus of σ_{hyd}) were determined from the analysis of XRD data [31]. It was found that σ_{hyd} is much smaller

(by ~25%) than σ_{bi} ; thus the effect of the biaxial compressive stress on the indentation cracks is predominant. Fig. 8 shows that the biaxial stress, determined by XRD in irradiated YSZ pellets [31], increases with increasing ion fluence, similarly to the fracture toughness. Actually, the residual stress field produced by radiation in the plane parallel to the sample surface is in compression and inhibits the crack propagation produced by the applied indentation load during the fracture toughness investigation (Fig. 9). The higher the stress intensity, the shorter the crack length and the higher the fracture toughness. The occurrence of a residual stress is then responsible for the increase of the toughness. A similar effect was observed by Motohashi et al. [17] in 3 mol% tetragonal YSZ polycrystals irradiated with 130 MeV Zr ions. Compressive residual stresses occurred in the surface region of irradiated specimens, and an increase of the hardness and of the fracture toughness were found.

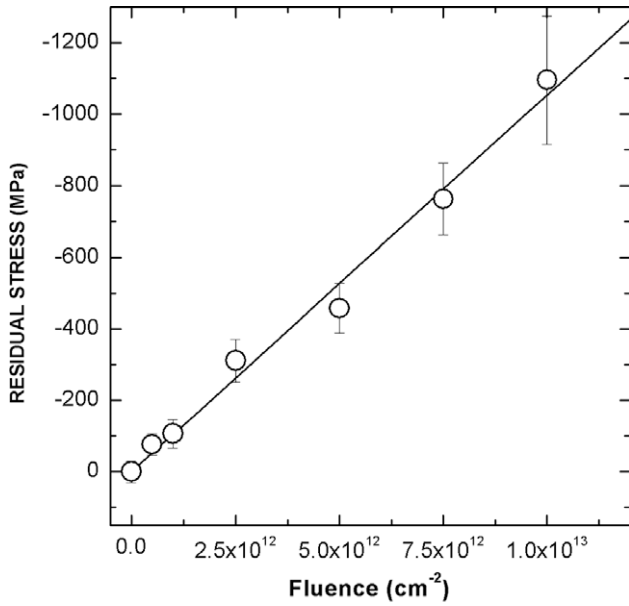


Fig. 8. Residual stress determined by XRD versus ion fluence (from [29]) for YSZ with a small grain size irradiated with 940 MeV Pb ions.

Since the surface of irradiated YSZ is subjected to residual stresses, the toughness measured by indentation is not the actual toughness of YSZ but it is only an effective fracture toughness. When a residual stress field is introduced into the surface, the total stress intensity factor K is given by [32–34]:

$$K = K_p + K_s, \quad (5)$$

where K_p is the stress intensity factor produced by an applied indentation load and K_s is the stress intensity factor due to the residual stress field. The cracks extend when K reaches a critical value K_{IC} (toughness) and Eq. (5) may be rewritten as:

$$K_{IC} = K_{IC}^{eff} + K_s, \quad (6)$$

where K_{IC}^{eff} is the effective fracture toughness measured by indentation, with $K_{IC}^{eff} = 0.0154 \left(\frac{E}{H_V}\right)^{1/2} \frac{P}{c^{3/2}}$ (see Eq. (2)).

If the residual biaxial stress σ_R is distributed uniformly, at least two interesting cases may be found according to the relative dimension of the crack size and of the layer depth (d) over which the stress acts [33]:

$$(i) \text{ if } c \approx d \text{ then } K_S = 2\sqrt{\frac{c}{\pi}}\sigma_R, \quad (7)$$

$$(ii) \text{ if } c \gg d \text{ then } K_S = 4\sqrt{\frac{d}{\pi}}\sigma_R. \quad (8)$$

However, in the present study we are in an intermediate case between Eqs. (7) and (8), since $26 \mu\text{m} \leq c \leq 43 \mu\text{m}$ and $d \approx R_p = 28 \mu\text{m}$. So, it is likely to assume that $K_S = \alpha\sigma_R$, where α is a positive constant. Eq. (6) can thus be rewritten as:

$$K_{IC} = K_{IC}^{eff} + \alpha\sigma_R. \quad (9)$$

Note that the occurrence of a surface stress is equivalent to a reduction or to an increase of the resistance to fracture, depending whether σ_R is tensile or compressive, respectively. In our study, we observed an increase of K_{IC}^{eff} with increasing ion fluence, so that irradiation generated compressive stresses leading to an increase of the effective toughness. Moreover, there is an interesting limit to the actual toughness K_{IC} . Here, we have $K_{IC}^{eff} > 0$, whereas $K_S < 0$ as $\sigma_R < 0$. Moreover, K_{IC}^{eff} and the absolute value of K_S increase with increasing fluence. So, K_{IC} can be reduced to zero. In this case, the crack size becomes infinite, corresponding to an unlimited and spontaneous extension of the cracks across the specimen surface. Above a fluence of 10^{13} cm^{-2} , some spontaneous cracking and collapse of indents are observed, as mentioned previously. Such a phenomenon indicates that the zero limit for K_{IC} is close, so that Eq. (9) reduces to:

$$\alpha\sigma_R = -K_{IC}^{eff}. \quad (10)$$

At a fluence of 10^{13} cm^{-2} , the biaxial stress is equal to -1100 MPa and $K_{IC}^{eff} = 4 \text{ MPa m}^{1/2}$. From these values we obtain a value of $3.64 \times 10^{-3} \text{ m}^{1/2}$ for α . Then, K_S is calculated from the stress value determined by XRD and presented in Fig. 8. As K_{IC}^{eff} corresponds to the toughness measured by indentation, the variation of the actual toughness of YSZ with the ion fluence can be determined from Eq. (9) and is presented in Fig. 10. For the sake of clarity, only results obtained on the samples with a small grain size are presented.

The actual toughness of YSZ clearly decreases with increasing ion fluence. Even if an apparent increase of the toughness is observed, due to the occurrence of residual stresses, the material is damaged by irradiation and consequently its toughness is reduced by radiation defects. Nevertheless, if the residual stresses are not too high (for instance around -500 MPa), irradiation remains beneficial for practical applications since the apparent fracture toughness is improved.

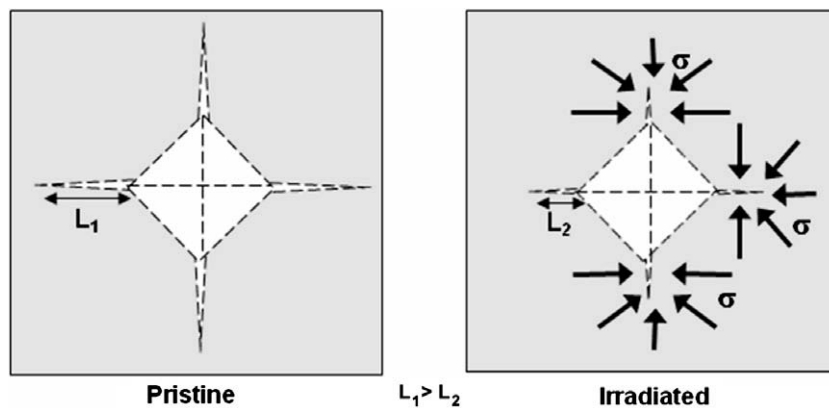


Fig. 9. Schematic illustration explaining the increase of the fracture toughness in YSZ polycrystals irradiated with 940 MeV Pb ions. Cracks initiate from the central deformation zone and develop along indentation diagonals. A residual compressive stress field opposes to crack propagation. Note that the crack length L_2 for an irradiated sample is smaller than the crack length L_1 for a pristine sample.

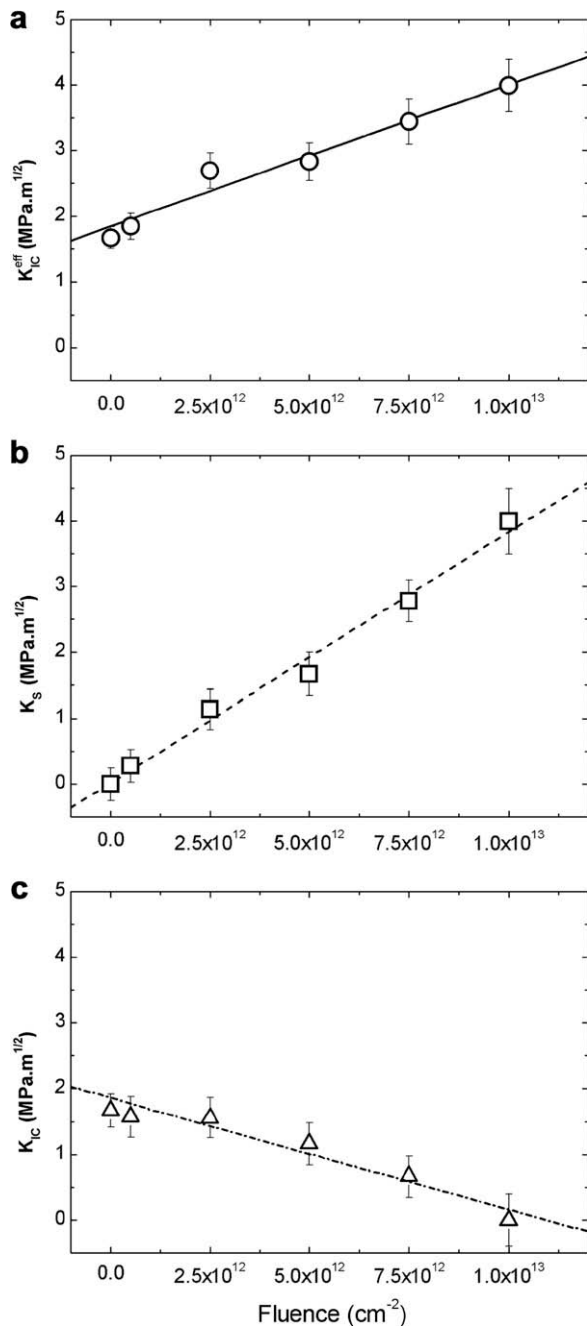


Fig. 10. Effective fracture toughness (a), absolute value of the intensity factor due to residual stress (b) and actual fracture toughness (c) versus ion fluence for YSZ with a small grain size irradiated with 940 MeV Pb ions.

5. Conclusion

The modifications of the mechanical properties of cubic yttria-stabilized zirconia polycrystals irradiated with swift heavy ions were investigated by Vickers micro-indentation associated to SEM and XRD. The results show that the measured values of the hardness and of the toughness of YSZ increase with increasing ion fluence.

Ion irradiation leads to the creation of both radiation defects and residual stresses in the surface layer of polycrystals. Since the presence of radiation damage should produce a decrease of

the toughness of YSZ, the occurrence of compressive residual stresses obviously over-compensates this effect, leading to the observed increase of the toughness of pellets upon irradiation.

Finally, the experiments reported in this paper demonstrate that swift heavy ion irradiation is an adequate technique for the strengthening of YSZ. The improvement of the mechanical properties of ceramics by ion irradiation is likely due to the fact that residual compressive stresses are introduced into the surface layer of samples. Therefore, ion irradiation may be used for materials processing with the goal of creating a reinforced surface layer, with a depth controlled by the ion beam energy, in order to overcome surface cracking or for tribological applications.

Acknowledgements

We thank A. Benyagoub for its assistance during swift heavy ion irradiations at GANIL. This work was partially supported by the GDR MATINEX.

References

- [1] C. Degueldre, U. Kasemeyer, F. Botta, G. Ledergerber, Mater. Res. Soc. Symp. Proc. 412 (1996) 15.
- [2] V.M. Oversby, C.C. McPheeters, C. Degueldre, J.M. Paratte, J. Nucl. Mater. 245 (1997) 17.
- [3] C. Degueldre, J.-M. Paratte, Nucl. Technol. 123 (1998) 21.
- [4] K.E. Sickafus, R.J. Hanrahan Jr., K.J. McClellan, J.N. Mitchell, C.J. Wetteland, D.P. Butt, P. Chodak III, K.B. Ramsey, H.T. Blair, K. Chidester, H. Matzke, K. Yasuda, R.A. Verrall, N. Yu, J. Am. Ceram. Soc. Bull. 78 (1) (1999) 69.
- [5] K.E. Sickafus, H. Matzke, T. Hartmann, K. Yasuda, J.A. Valdez, P. Chodak III, M. Nastasi, R.A. Verrall, J. Nucl. Mater. 274 (1999) 66.
- [6] W.L. Gong, W. Lutze, R.C. Ewing, J. Nucl. Mater. 277 (2000) 239.
- [7] D.F. Carroll, J. Am. Ceram. Soc. 46 (1963) 195.
- [8] I. Cohen, B.E. Schaner, J. Nucl. Mater. 9 (1963) 18.
- [9] F.A. Mumpton, R. Rustum, J. Am. Ceram. Soc. 43 (1960) 237.
- [10] N. Yu, K.E. Sickafus, P. Kodali, M. Nastasi, J. Nucl. Mater. 244 (1997) 266.
- [11] K. Yasuda, M. Nastasi, K.E. Sickafus, C.J. Maggiore, N. Yu, Nucl. Instrum. and Meth. B 136–138 (1998) 499.
- [12] N. Sasajima, T. Matsui, K. Hojou, S. Furuno, H. Otsu, K. Izui, T. Muromura, Nucl. Instrum. and Meth. B 141 (1998) 487.
- [13] L. Thomé, J. Fradin, J. Jagielski, A. Gentils, S.E. Enescu, F. Garrido, Eur. Phys. J. Appl. Phys. 24 (2003) 37.
- [14] G. Sattonnay, L. Thomé, J. Nucl. Mater. 348 (2006) 223.
- [15] K.E. Sickafus, C.J. Wetteland, N.P. Baker, N. Yu, R. Devanathan, M. Nastasi, N. Bordes, Mater. Sci. Eng. A 253 (1998) 78.
- [16] L. Boudoukha, S. Paletto, F. Halitim, G. Fantozzi, Nucl. Instrum. and Meth. B 122 (1997) 233.
- [17] Y. Motohashi, T. Kobayashi, S. Harjo, T. Sakuma, T. Shibata, M. Ishihara, S. Baba, T. Hoshiya, Nucl. Instrum. and Meth. B 206 (2003) 144.
- [18] V. Menvie Bekale, C. Legros, C. Haut, G. Sattonnay, A.M. Huntz, Solid State Ionics 177 (2006) 3339.
- [19] J.F. Ziegler, J.P. Biersack, U. Littmark, The Stopping and Range of Ions in Solids, Pergamon, New York, 1985.
- [20] G. Sattonnay, M. Lahrachi, A. Benyagoub, J.M. Costantini, F. Garrido, L. Thomé, C. Trautmann, Nucl. Instrum. and Meth. B 257 (2007) 476.
- [21] F.A. McClintock, A.S. Argon, Mechanical Behaviour of Materials, Addison-Wesley Publishing Company, Massachusetts, USA, 1966.
- [22] G.R. Anstis, P. Chantikul, B.R. Lawn, D.B. Marshall, J. Am. Ceram. Soc. 64 (1981) 539.
- [23] W.C. Oliver, G.M. Pharr, J. Mater. Res. 7 (1992) 1564.
- [24] M.F. Doerner, W.D. Nix, J. Mater. Res. 4 (1986) 601.
- [25] B. Eigenmann, B. Scholtes, E. Macherauch, Mat. -wiss. u. Werkstofftech. 20 (1989) 314.
- [26] G.A. Gogotsi, S.N. Dub, E.E. Lomonova, B.I. Ozersky, J. Eur. Ceram. Soc. 15 (1995) 405.
- [27] L. Donzel, S.G. Roberts, J. Eur. Ceram. Soc. 20 (2000) 2457.
- [28] P. Dahl, I. Kaus, Z. Zhao, M. Johnsson, M. Nygren, K. Wiik, T. Grande, M.A. Einarsrud, Ceram. Int. 33 (2007) 1603.
- [29] J.F. Knott, Fundamentals of Fracture Mechanics, John Wiley-Halsted Press, New York, 1973.
- [30] S. Moll et al., J Appl. Phys. (2008) in press.
- [31] G. Sattonnay, M. Lahrachi, M. Herbst-Ghysel, F. Garrido, L. Thomé, J. Appl. Phys. 101 (2007) 103516.
- [32] D.B. Marshall, B.R. Lawn, J. Am. Ceram. Soc. 60 (1980) 86.
- [33] B.R. Lawn, E.R. Fuller, J. Mater. Res. 19 (1984) 4061.
- [34] T.-Y. Zhang, L.-Q. Chen, R. Fu, Acta Mater. 14 (1999) 3869.